Insulator-protected mechanically controlled break junctions for measuring single-molecule conductance in aqueous environments

Muthusubramanian, N.; Galan, E.; Maity, C.; Eelkema, R.; Grozema, F. C.; Van Der Zant, H. S J

DOI
10.1063/1.4955273

Publication date
2016

Document Version
Final published version

Published in
Applied Physics Letters

Insulator-protected mechanically controlled break junctions for measuring single-molecule conductance in aqueous environments

N. Muthusubramanian, E. Galan, C. Maity, R. Eelkema, F. C. Grozema, and H. S. J. van der Zant

Citation: Appl. Phys. Lett. **109**, 013102 (2016); doi: 10.1063/1.4955273
View online: http://dx.doi.org/10.1063/1.4955273
View Table of Contents: http://aip.scitation.org/toc/apl/109/1
Published by the American Institute of Physics

Insulator-protected mechanically controlled break junctions for measuring single-molecule conductance in aqueous environments

N. Muthusubramanian,[1] E. Galan,[2] C. Maity,[2] R. Eelkema,[2] F. C. Grozema,[2] and H. S. J. van der Zant[1]
[1]*Kavli Institute of Nanoscience, Delft University of Technology, Lorentzweg 1, 2628 CJ Delft, The Netherlands*
[2]*Department of Chemical Engineering, Delft University of Technology, Van der Maasweg 9, 2629 HZ Delft, The Netherlands*

(Received 2 May 2016; accepted 23 June 2016; published online 5 July 2016)

We present a method to fabricate insulated gold mechanically controlled break junctions (MCBJ) by coating the metal with a thin layer of aluminum oxide using plasma enhanced atomic layer deposition. The Al_2O_3 thickness deposited on the MCBJ devices was varied from 2 to 15 nm to test the suppression of leakage currents in deionized water and phosphate buffered saline. Junctions coated with a 15 nm thick oxide layer yielded atomically sharp electrodes and negligible conductance counts in the range of 1 to 10^{-4} G_0 ($1\ G_0 = 77\ \mu S$), where single-molecule conductances are commonly observed. The insulated devices were used to measure the conductance of an amphiphilic oligophenylene ethynylene derivative in deionized water. *Published by AIP Publishing.*
[http://dx.doi.org/10.1063/1.4955273]

The field of molecular electronics provides a versatile testbed for studying the electronic properties of single molecules, including quantum interference effects,[1–3] tuning of charge transport by electrochemistry,[4–8] interactions with environmental variables such as pH,[9,10] solvent induced effects,[11–14] and charge transport in biological moieties.[15–19] Over the past decade, such charge transport measurements through single molecules have been conducted with metallic break junctions formed by means of scanning probe or nanolithography techniques; with scanning tunnelling microscopy being an example for the former and mechanically controlled break junctions (MCBJ) for the latter. Both break junction techniques can be operated at room temperature, although research on the role of environmental variables such as solvent interactions and electrochemical gating has not received the same level of attention for the MCBJ approach[20–24] compared to the STM method.[25–28] Measurements in polar solvents give rise to faradaic leakage currents which may exceed the conductance of the molecule of interest; hence, the electrodes must be sufficiently insulated to reduce this parasitic current ideally below the noise level. The advantages of STM break junctions is the simplicity and larger dimensions of the source and drain electrodes. Structural modifications such as applying an electrically insulating layer over STM tips for measurements in polar and electrolytic solutions are a relatively facile process.[29]

Due to the planar architecture and nano-scale electrode dimensions of the lithographically fabricated electrodes, alternative insulation techniques must be developed to insulate the MCBJ devices. Such insulated MCBJ would then combine the advantages of high mechanical stability, symmetry of source-drain electrodes, and different measurement routines such as self-breaking[30–32] with the ability to investigate the effects of solvents on conductance of various molecular systems. The work by Arima et *al.*[33] describes the use of SiO_2 as their choice of the dielectric material deposited on MCBJ devices by chemical vapor deposition (CVD) to suppress leakage currents in aqueous solutions. However, they did not demonstrate the ability to measure single-molecule conductance using the SiO_2-coated MCBJ devices.

In this letter, we report the use of aluminum oxide deposited by means of plasma enhanced atomic layer deposition (ALD) as the dielectric material for insulating MCBJ electrodes. The choice of Al_2O_3 is based on its excellent mechanical and dielectric properties, chemical stability within the pH range 3–10, and the ability to deposit thin films in an isotropic manner of high purity by means of ALD. Measurements using MCBJ devices coated with 15 nm oxide layer show characteristic features that closely resemble those of the bare-gold reference samples. In our Al_2O_3 insulated devices, we have also measured metal-molecule-metal junctions in deionized (DI) water using a thioacetate-terminated oligophenylene ethynylene (OPE3) functionalized with hydrophilic polyethylene oxide side chains. Due to the simple conjugated structure and substantive literature on conductance measurements[22,34–37] of OPE3 analogs, it was considered as a model system for testing the working of the insulator-modified mechanically controlled break junctions in solution environment.

Mechanically controlled break junction (MCBJ) devices were fabricated by spin-coating a transparent and flexible insulating layer of polyimide (HD Microsystems, PI-2600 series) on polished phosphor bronze substrates. The electrodes were patterned as a thin wire using electron-beam lithography followed by deposition of a chromium adhesion layer and finally gold of thickness 4 and 80 nm, respectively. The center of the thin wire was constricted to facilitate the formation of two sharp electrodes upon mechanical actuation in the measurement setup. The gold wires were suspended over a length of 1 μm by etching the underlying polyimide layer using a mixture of O_2/CF_4 plasma.[38]

Finally, the devices were coated with a thin layer of Al_2O_3 of nominal thicknesses varying from 2 to 15 nm using plasma enhanced ALD at a temperature of 300 °C using a

FlexAL® ALD system from Oxford Instruments. A nominal thickness of 15 nm corresponds to 150 ALD cycles, and the corresponding layer thickness was measured to be between 16 and 17 nm for different runs; in this paper, we list the nominal thickness value as set by the number of ALD cycles. Scanning electron microscopy and energy dispersive X-ray spectroscopy analysis of the MCBJ devices coated with different oxide thicknesses are presented in the supplementary material.[39] For solution-based measurements, commercial Press-to-Seal® silicone gaskets of 2 mm diameter and with an effective volume of 20 μl were placed on top of the devices and covered with a clean adhesive foil to prevent solvent evaporation. Figure 1(a) shows the scheme and working principle of the MCBJ device with a liquid cell mounted on top, while Figure 1(b) depicts a scanning electron microscope image of a suspended Au wire coated with Al_2O_3 by 150 ALD cycles.

Measurements are carried out at room temperature using a home-built mechanically controlled break junction setup, details of which have been described elsewhere.[40] Break junctions are formed *in-situ* by controlled actuation of the MCBJ device in a three-point bending mechanism. The cyclical junction breaking and formation routine is achieved by means of a feedback-controlled piezoelectric stack actuator with an attenuated vertical to horizontal displacement ratio of about 5×10^{-5}.[38] A DC bias of 0.1 V is applied across the junction while the conductance is measured from 10 G_0 to below 10^{-7} G_0 using a home-built logarithmic amplifier. Here, G_0 is the conductance quantum $G_0 = 2e^2/h$, where e is charge of the electron and h is Planck's constant. Measurements are performed using an electrode displacement rate ranging from 2 to 6 nm s^{-1} with the nanogap stretched over 6 nm during the breaking process. For each experiment prior to the deposition of molecules on the break junctions, reference measurements with the bare MCBJ device are carried out to check the cleanness of the gold junctions and to calibrate the electrode displacement (Δz) corresponding to the voltage applied on the piezoelectric actuator (V_p). The method to calculate this calibration factor has been described in the supplementary material.[39] The raw data acquired from the measurements are in the form of conductance vs time traces, which are represented as a function of electrode displacement in two-dimensional conductance histograms. All one and two-dimensional conductance histograms presented in this work are derived from more than one thousand consecutive conductance traces per dataset without data selection.

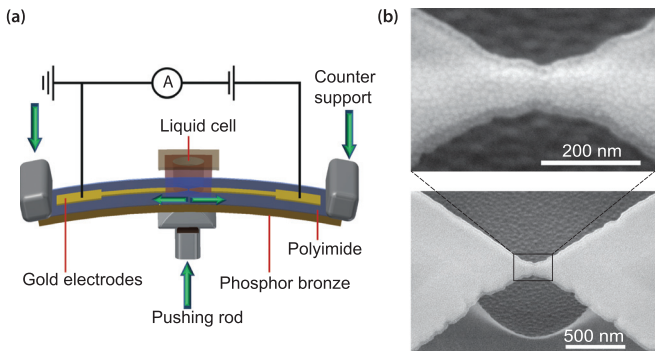

FIG. 1. (a) Schematic of the working principle of a mechanically controlled break junction (MCBJ) with a liquid cell. (b) Scanning electron microscope images of an MCBJ device coated with Al_2O_3 deposited by 150 ALD cycles (thickness is 15 nm). Bottom panel: Suspended part of the gold bridge imaged at 45° tilt. Top panel: Magnified view of the constricted area.

We first characterized non-insulated MCBJ devices measured in dry ambient conditions and in deionized water (DI H_2O) of resistivity 14.2 MΩ cm at 20 °C as shown in Figure 2. The one-dimensional conductance histograms in Figure 2(b) show clear peaks near 1 G_0, indicating the formation of atomically sharp contacts in the aforementioned conditions. A distinct difference is observed at low conductance values in both the one and two-dimensional histograms; the measurements in DI H_2O display leakage currents which decay to a conductance level in the order of 10^{-5} G_0. These observations indicate that the signatures of molecules with sub-10^{-4} G_0 conductance values can be masked by leakage currents through solvents, making measurements with non-insulated electrodes challenging.

Similar measurements in DI H_2O have been performed with Al_2O_3 coated devices with nominal oxide thicknesses ranging from 2 to 15 nm. The corresponding conductance histograms for four different oxide thicknesses are compared in Figure 3. At least two devices per thickness were investigated; the data in the figure present typical examples. The MCBJ devices coated with 2 nm Al_2O_3 still show leakage currents, whereas for the devices coated with Al_2O_3 of thickness 5 nm and above the leakage currents have dropped below 10^{-6} G_0. The formation of a well-defined 1 G_0 peak was observed in all 1-D conductance histograms in Figure 3(b), indicating the

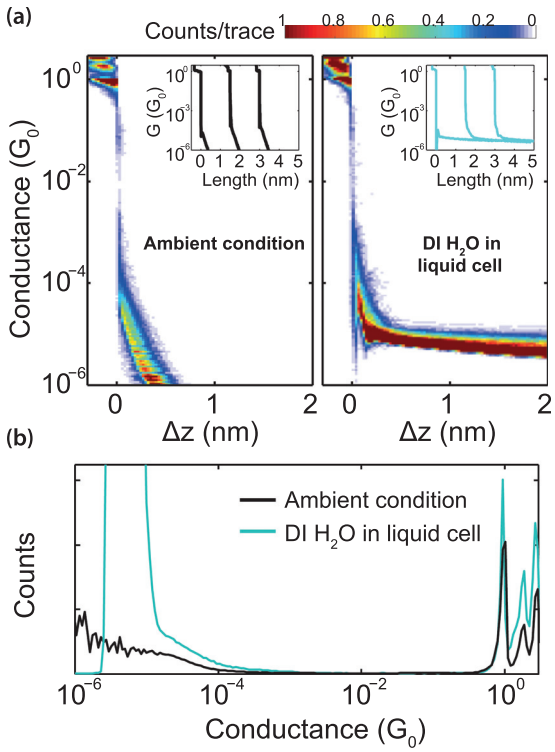

FIG. 2. (a) Two-dimensional histograms of conductance vs electrode separation with an applied bias of 0.1 V, binning values of 75 bins/nm along the x-axis and 33 bins/decade along the y-axis, and electrode displacement rate of 6 nm s^{-1} for measurements using bare non-insulated MCBJ device in dry ambient conditions (left panel) and 2 nm s^{-1} for measurements in deionized water (right panel). The insets show single traces of the corresponding datasets. (b) A comparison of the corresponding one-dimensional conductance histograms.

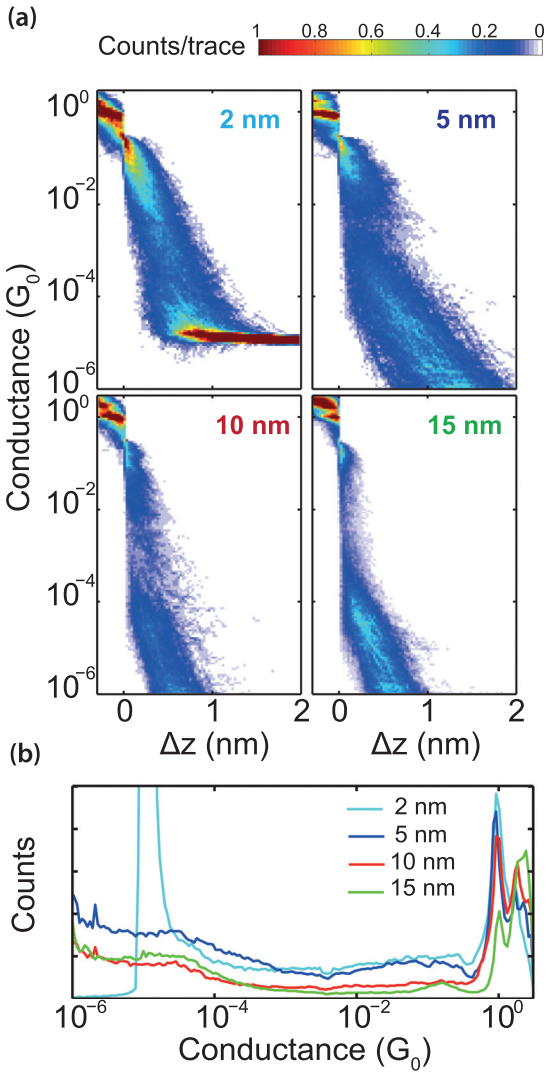

FIG. 3. (a) Two-dimensional conductance histograms of MCBJ devices measured in DI H_2O insulated with Al_2O_3 using plasma enhanced atomic layer deposition of different thickness values. (b) The corresponding one-dimensional conductance histograms of the insulated devices.

formation of atomic point contacts even after depositing a thin layer of the dielectric material on the gold surface.

Another important aspect for using the MCBJ technique to measure the conductance of single molecules is a minimal occurrence of conductance counts below 1 G_0 until the conductance value for which tunnelling sets in, which is typically at 10^{-4} G_0 in our devices. As shown in Figure 3(a) upper panels, the Al_2O_3-coated devices of oxide thicknesses below 10 nm show substantial number of counts in this range of conductance, making these devices unsuitable for a clear distinction of the presence of single-molecule features and the determination of their conductance. However, for the MCBJ device coated with Al_2O_3 of nominal thickness 15 nm, the number of counts is low, and the 2-D histogram appears to be featureless. It is also important to note that for the 15 nm insulated device, the tunnelling decay with distance below 10^{-4} G_0 is similar to that of the bare-gold reference (Figure 2(a), left panel). This clean behavior was found to be reproducible in 50% of the 15 nm Al_2O_3-coated devices measured. The physical robustness of the 15 nm Al_2O_3-coated devices was also corroborated by measuring more than 10 000 consecutive traces in DI H_2O to probe the time evolution of the break junctions.[39] Such measurements can also be used to calibrate the displacement ratio prior to drop-casting the molecule of interest as mentioned earlier.

The insulated devices were tested in a solution of phosphate buffered saline (PBS) of concentrations 1 to 10 mM of pH 7.4, which is a commonly used buffer for biological techniques such as DNA extraction and cell culture. The conductance histograms of a non-insulated MCBJ device measured in 10 mM PBS solution shows leakage currents decaying to a conductance level of 10^{-4} to 10^{-5} G_0, an order of magnitude higher than that observed in DI H_2O. Measurements with a 15 nm Al_2O_3-coated device in the buffer show suppression of leakage currents below 10^{-5} G_0.[39] Additionally, above this conductance value, the spread of conductance counts with respect to the electrode displacement is lesser than 0.5 nm, which bears a similarity to the bare gold reference.

To test the feasibility of measuring single-molecule conductance in aqueous solution using MCBJ devices coated with a 15 nm thick insulating layer, we test the water-soluble OPE3-PEO derivative as shown in Figure 4(a) (for details of synthesis, see the supplementary material).[39] The molecule was dissolved in deionized water (0.1 mM, 1 ml) and added into the liquid cell attached to the device. Prior to starting the measurements, 100 μl of a 2 mM aqueous solution of tetrabutylammonium hydroxide 30-hydrate (Sigma-Aldrich) was added into the liquid cell to deprotect the thiol groups of the molecule. In the case of conductance histograms with the OPE3-PEO molecule in aqueous environment, as illustrated in Figure 4(b), there is a region of high conductance counts with the most probable conductance of 1.3×10^{-5} G_0 obtained by a Gaussian function. Single traces from the 2-D conductance histogram (Figure 4(b) inset) shows plateau-like feature whose length corresponds to the molecular length of OPE3-PEO. Measurements with the OPE3-PEO molecule were repeated using five insulated devices, which gave similar conductance values. Further research on the comparison of conductance values of OPE3-based molecules in dry conditions and in aqueous solutions is currently being investigated.

In conclusion, we developed a method to study the effects of an aqueous environment on charge transport in single molecules using Al_2O_3 protected mechanically controlled break junctions. We found that atomically sharp point

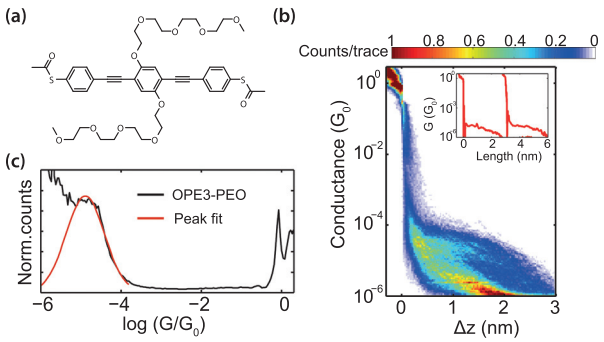

FIG. 4. (a) Chemical structure of the water-soluble OPE3-PEO molecule. (b) Two-dimensional conductance histogram of deprotected OPE3-PEO measured in DI H_2O using a 15 nm Al_2O_3 insulated device. (c) The corresponding one-dimensional conductance histogram of OPE3-PEO with peak fitting yielding a conductance value of 1.3×10^{-5} G_0.

contacts are formed using such oxide-coated devices and that the spread of conductance counts between 1 and 10^{-4} G_0 for the case of the 15 nm oxide thickness is very similar to that of a bare gold reference sample. Measurements in aqueous buffer solutions and with the amphiphilic OPE3-PEO molecule dissolved in water show the potential of this technique to obtain statistically relevant data in solvent environments.

This research was supported by the EU Marie Curie Initial Training Network (ITN) "Molecular-Scale Electronics" MOLESCO, Project No. 606728. N.M. acknowledges M.L. Perrin for discussions about insulation techniques for the mechanically controlled break junction devices.

[1]C. M. Guedon, H. Valkenier, T. Markussen, K. S. Thygesen, J. C. Hummelen, and S. J. v. d. Molen, Nat. Nanotechnol. **7**, 305 (2012).
[2]C. R. Arroyo, S. Tarkuc, R. Frisenda, J. S. Seldenthuis, C. H. M. Woerde, R. Eelkema, F. C. Grozema, and H. S. J. v. d. Zant, Angew. Chem. **125**, 3234 (2013).
[3]A. Batra, J. S. Meisner, P. Darancet, Q. Chen, M. L. Steigerwald, C. Nuckolls, and L. Venkataraman, Faraday Discuss. **174**, 79 (2014).
[4]X. Xiao, B. Xu, and N. J. Tao, Nano Lett. **4**, 267 (2004).
[5]X. Li, J. He, J. Hihath, B. Xu, S. M. Lindsay, and N. J. Tao, J. Am. Chem. Soc. **128**, 2135 (2006).
[6]F. Chen, J. He, C. Nuckolls, T. Roberts, J. E. Klare, and S. M. Lindsay, Nano Lett. **5**, 503 (2005).
[7]Z. Li, Y. Liu, S. F. L. Mertens, I. V. Pobelov, and T. Wandlowski, J. Am. Chem. Soc. **132**, 8187 (2010).
[8]B. Capozzi, Q. Chen, P. Darancet, M. Kotiuga, M. Buzzeo, J. B. Neaton, C. Nuckolls, and L. Venkataraman, Nano Lett. **14**, 1400 (2014).
[9]L. Scullion, T. Doneux, L. Bouffier, D. G. Fernig, S. J. Higgins, D. Bethell, and R. J. Nichols, J. Phys. Chem. C **115**, 8361 (2011).
[10]Z. Li, M. Smeu, S. Afsari, Y. Xing, M. A. Ratner, and E. Borguet, Angew. Chem. **126**, 1116 (2014).
[11]E. Leary, H. Hobenreich, S. J. Higgins, H. van Zalinge, W. Haiss, R. J. Nichols, C. M. Finch, I. Grace, C. J. Lambert, R. McGrath, and J. Smerdon, Phys. Rev. Lett. **102**, 086801 (2009).
[12]V. Fatemi, M. Kamenetska, J. B. Neaton, and L. Venkataraman, Nano Lett. **11**, 1988 (2011).
[13]M. Kotiuga, P. Darancet, C. R. Arroyo, L. Venkataraman, and J. B. Neaton, Nano Lett. **15**, 4498 (2015).
[14]D. C. Milan, O. A. Al-Owaedi, M.-C. Oerthel, S. Marques-Gonzalez, R. J. Brooke, M. R. Bryce, P. Cea, J. Ferrer, S. J. Higgins, C. J. Lambert, P. J. Low, D. Z. Manrique, S. Martin, R. J. Nichols, W. Schwarzacher, and V. M. Garcia-Suarez, J. Phys. Chem. C (published online, 2015).
[15]B. Xu, P. Zhang, X. Li, and N. J. Tao, Nano Lett. **4**, 1105 (2004).
[16]X. Xiao, B. Xu, and N. J. Tao, J. Am. Chem. Soc. **126**, 5370 (2004).
[17]A. Alessandrini, S. Corni, and P. Facci, Phys. Chem. Chem. Phys. **8**, 4383 (2006).
[18]S. Sek, A. Misicka, K. Swiatek, and E. Maicka, J. Phys. Chem. B **110**, 19671 (2006).
[19]Y.-S. Chen, M.-Y. Hong, and G. S. Huang, Nat. Nanotechnol. **7**, 197 (2012).
[20]L. Gruter, M. T. Gonzalez, R. Huber, M. Calame, and C. Schonenberger, Small **1**, 1067 (2005).
[21]L. Gruter, F. Cheng, T. T. Heikkila, M. T. Gonzalez, F. Diederich, C. Schonenberger, and M. Calame, Nanotechnology **16**, 2143 (2005).
[22]R. Huber, M. T. Gonzalez, S. Wu, M. Langer, S. Grunder, V. Horhoiu, M. Mayor, M. R. Bryce, C. Wang, R. Jitchati, C. Schonenberger, and M. Calame, J. Am. Chem. Soc. **130**, 1080 (2008).
[23]W. Hong, H. Valkenier, G. Meszaros, D. Z. Manrique, A. Mishchenko, A. Putz, P. M. Garcia, C. J. Lambert, J. C. Hummelen, and T. Wandlowski, Beilstein J. Nanotechnol. **2**, 699 (2011).
[24]D. Xiang, H. Jeong, T. Lee, and D. Mayer, Adv. Mater. **25**, 4845 (2013).
[25]N. J. Tao, Nat. Nanotechnol. **1**, 173 (2006).
[26]X. Li, B. Xu, X. Xiao, X. Yang, L. Zang, and N. J. Tao, Faraday Discuss. **131**, 111 (2006).
[27]J. Hihath, F. Chen, P. Zhang, and N. J. Tao, J. Phys.: Condens. Matter **19**, 215202 (2007).
[28]J. Zhang, A. M. Kuznetsov, I. G. Medvedev, Q. Chi, T. Albrecht, P. S. Jensen, and J. Ulstrup, Chem. Rev. **108**, 2737 (2008).
[29]L. A. Nagahara, T. Thundat, and S. M. Lindsay, Rev. Sci. Instrum. **60**, 3128 (1989).
[30]K. O'Neill, E. A. Osorio, and H. S. J. v. d. Zant, Appl. Phys. Lett. **90**, 133109 (2007).
[31]Z. Huang, F. Chen, P. A. Bennett, and N. J. Tao, J. Am. Chem. Soc. **129**, 13225 (2007).
[32]M. Tsutsui, K. Shoji, K. Morimoto, M. Taniguchi, and T. Kawai, Appl. Phys. Lett. **92**, 223110 (2008).
[33]A. Arima, M. Tsutsui, T. Morikawa, K. Yokota, and M. Taniguchi, J. Appl. Phys. **115**, 114310 (2014).
[34]M. T. Gonzalez, E. Leary, R. Garcia, P. Verma, M. A. Herranz, G. Rubio-Bollinger, N. Martin, and N. Agrait, J. Phys. Chem. C **115**, 17973 (2011).
[35]R. Frisenda, M. L. Perrin, H. Valkenier, J. C. Hummelen, and H. S. J. v. d. Zant, Phys. Status Solidi B **250**, 2431 (2013).
[36]C. Huang, A. V. Rudnev, W. Hong, and T. Wandlowski, Chem. Soc. Rev. **44**, 889 (2015).
[37]R. Frisenda, S. Tarkuc, E. Galan, M. L. Perrin, R. Eelkema, F. C. Grozema, and H. S. J. v. d. Zant, Beilstein J. Nanotechnol. **6**, 1558 (2015).
[38]C. A. Martin, D. Ding, H. S. J. v. d. Zant, and J. M. v. Ruitenbeek, New J. Phys. **10**, 065008 (2008).
[39]See supplementary material at http://dx.doi.org/10.1063/1.4955273 for chemical synthesis of OPE3-PEO molecule, SEM and EDX analysis of the MCBJ devices, length calibration analysis, time evolution and measurements of insulated break junctions in buffer solutions.
[40]C. A. Martin, R. H. M. Smit, R. v. Egmond, H. S. J. v. d. Zant, and J. M. v. Ruitenbeek, Rev. Sci. Instrum. **82**, 053907 (2011).